Nonagostic M···H−C Interactions. Synthesis, Characterization, and DFT Study of the Titanium Amide Ti2Cl6[N(t−Bu)2]2

ARTICLE *in* ORGANOMETALLICS · JUNE 2012

Impact Factor: 4.13 · DOI: 10.1021/om300483v

ORGANOMETALLICS

Article

pubs.acs.org/Organometallics

Nonagostic M···H−C Interactions. Synthesis, Characterization, and DFT Study of the Titanium Amide $Ti_2Cl_6[N(t\text{-}Bu)_2]_2$

Charles W. Spicer, Charity Flener Lovitt, and Gregory S. Girolami*

School of Chemical Sciences, University of Illinois at Urbana−Champaign, 600 South Mathews Avenue, Urbana, Illinois 61801, United States

Supporting Information

ABSTRACT: The compound $Ti_2Cl_6[N(t\text{-}Bu)_2]_2$ (**1**) has been synthesized by treating $TiCl_4$ with di(*tert*-butyl)amine, $HN(t\text{-}Bu)_2$. Compound **1** crystallizes in two different polymorphs from pentane, both conforming to the space group $P2_1/n$. In both polymorphs, **1** exhibits a close Ti···C contact of 2.634(3) Å between titanium and a γ-methyl group in one of the two *tert*-butyl groups of the bound amido ligand. Interestingly, the γ-methyl group adopts a rotational conformation that maximizes the Ti···H distances, the shortest of which are 2.36(2) and 2.62(2) Å. Even though the former distance is within the range characteristic of agostic interactions, the rotational orientation of the methyl group suggests that the Ti···H interactions are repulsive rather than attractive. DFT and NBO analysis confirms this supposition: there is no evidence of weakening of the C−H bond closest to the titanium and no evidence of significant overlap of titanium orbitals with the C−H bonding orbitals of the γ-methyl group involved in the close contact. Further evidence that the close contact is repulsive was obtained from a DFT study of a series of related complexes in which the $N(t\text{-}Bu)_2$ ligand is replaced with a $NR(t\text{-}Bu)$ ligand, where the substituent R not involved in the close contact is Et, Me, or $SiMe_3$. All of these latter substituents, which are sterically smaller than a *t*-Bu group, enable the amide group to pivot in such a way as to move the *tert*-butyl group farther from the metal center. The results suggest that the short Ti···C and Ti···H distances seen crystallographically for **1** are actually the result of intraligand and interligand steric repulsions involving the amide substituent not involved in the close contact. The lack of an agostic interaction despite the close contact (and the low electron count of the Ti center) is ascribed to the strong σ- and π-donor properties of the amide and chloride ligands, which raise the energies of the empty orbitals on Ti.

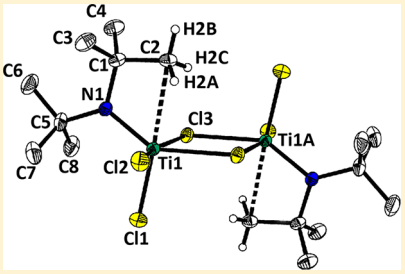

INTRODUCTION

Since the word "agostic" was coined in 1983 as a term for three-center−two-electron interactions involving a metal and a carbon−hydrogen bond,[1] agostic interactions have been found to play an important role in organometallic chemistry, being present, for example, in key intermediates in Ziegler−Natta catalysts for the polymerization of alkenes. From a structural viewpoint, agostic interactions can be classified as α, β, γ, etc., according to the location of the interacting C−H bond relative to the metal center.[2−6] Detailed studies suggest that α-agostic interactions form in order to maximize the metal−carbon orbital overlap, whereas β- and more remote interactions with C−H bonds maximize metal−hydrogen overlap.[4,7−10]

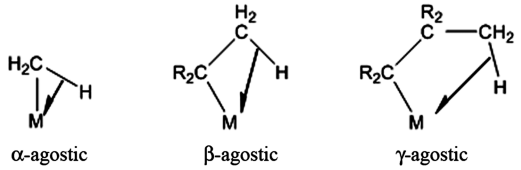

Complexes that exhibit γ-agostic geometries are less common than those that contain α- and β-geometries.[11−15] Although the presence of γ-C−H agostic interactions is usually determined crystallographically, their presence can also be inferred from NMR chemical shifts[16] and kinetic isotope studies.[17]

Metal complexes of bulky ligands bearing trimethylsilyl groups, such as the alkyl $CH(SiMe_3)_2$ and the amide $N(SiMe_3)_2$, often form what appear at first glance to be γ-agostic interactions (Table 1). In a few cases, such as for the complexes $(C_5Me_5)_2Y[N(SiMe_3)_2]$ and $(C_5Me_5)_2Y[CH(SiMe_3)_2]$, the X-ray crystal structures show that a hydrogen atom on a γ-carbon points directly at the metal center, forming an unusually short M−H contact.[18] In most other complexes containing close contacts to atoms in these silylated ligands, however, the structural feature is due not to an agostic interaction with a C−H group but rather to M···Si−C interactions instead. Perhaps the best studied example of the latter situation is the compound $(C_5Me_5)La[CH(SiMe_3)_2]_2$, whose crystal structure indicated that the La center forms a close contact of only 2.988(6) Å with one of the γ-carbon atoms and a close contact of 3.353(2) Å with the associated silicon atom.[19,20] Although solid-state ^1H and ^{13}C NMR studies were unable to determine whether the γ-agostic interaction or the M−Si interaction was more important to the bonding,[21] later neutron diffraction studies revealed that the γ-C−H bond length in $(C_5Me_5)La[CH(SiMe_3)_2]_2$ is unchanged from its normal value.[22] Similar behavior was also found for the yttrium complex $(C_5Me_5)Y(OC_6H_3(t\text{-}Bu)_2)[CH(SiMe_3)_2]$,

Received: May 31, 2012
Published: June 19, 2012

   dx.doi.org/10.1021/om300483v | *Organometallics* 2012, 31, 4894−4903

Table 1. Structural Data for Complexes with γ-Agostic and Related Interactions

molecule	contact	interaction distance (Å)	ref
$RuCl_2(PPh_3)[N(SiMe_3)CPhNH(PPh_2)]$	Ru−γ-C	3.16	13
$[Cp_2Ti(C(SiMe_3)=CMePh)][AlCl_4]$	Ti−γ-C	2.52	11, 12
$Sr[N(2,4,6\text{-}Me_3C_6H_2)(SiMe_3)]_2(PMDTA)$	Sr−γ-H	2.90	14
$Li_2[N(t\text{-}Bu)SiMe_2(C_6H_4OMe)]_2$	Li−γ-H	2.56	15
$Li_2[N(t\text{-}Bu)SiMe_2(C_6H_4NMe_2)]_2$	Li−γ-H	2.68	15
$Li_2[N(t\text{-}Bu)SiMe_2(C_6H_4CH_2NMe_2)]_2$	Li−γ-H	2.79	15
$Li_2[N(t\text{-}Bu)SiMe_2(C_6H_4CF_3)]_2$	Li−γ-H	2.42	15
$(C_5Me_5)Y(OC_6H_3(t\text{-}Bu)_2)[CH(SiMe_3)_2]$	Y−γ-C	2.97	22
$(C_5Me_5)_2Y[N(SiMe_3)_2]$	Y−γ-H	2.45	18
$(C_5Me_5)_2Y[CH(SiMe_3)_2]$	Y−γ-H	2.45	18
$(C_5Me_5)La[CH(SiMe_3)_2]_2$	La−γ-C	2.96	19−22
$Sm[N(SiMe_3)_2]_3$	Sm−γ-C	3.00	27
$Sm[N(SiMe_3)_2]_2(THF)_2$	Sm−γ-C	3.32	28
$Sm_2[N(SiMe_3)_2]_2(DME)_2(THF)_2$	Sm−γ-C	3.37	28
$Yb[N(SiMe_3)_2]_2(AlMe_3)_2$	Yb−γ-C	2.76	30
$Yb[N(SiMe_3)_2]_2(DMPE)$	Yb-γ-C	3.04	31
$NaYb[N(SiMe_3)_2]_3$	Yb−γ-C	2.86	29
$NaEu[N(SiMe_3)_2]_3$	Eu−γ-C	3.04	29
$U(S\text{-}2,6\text{-}Me_2C_6H_3)[N(SiMe_3)_2]_3$	U−γ-C	3.23	32, 33
$U[CH(SiMe_3)_2]_3$	U−γ-C	3.09	24

which also contains a close contact with a γ-C−H bond of a $CH(SiMe_3)_2$ ligand.[22] In addition, the hydrogen atoms bound to the γ-carbon are oriented in a fashion to maximize their distances to the metal center. The data strongly suggest that, in both these compounds, there is no agostic M···H−C interaction, but that instead electrons from the Si−C bond donate in a sigma fashion to the metal center.[22] The compounds $Ln[CH(SiMe_3)_2]_3$, $Sm[CH(SiMe_3)_2]_3$, and $U[CH(SiMe_3)_2]_3$ also show evidence of close contacts between the metal center and Si−C bonds.[23,24] DFT calculations lend support to the conclusion that the Si−C bond is a sigma donor toward the respective metal centers and that no γ-agostic interactions are present.[25,26]

Similar close contacts have also been observed in $-N(SiMe_3)_2$ compounds of samarium,[27,28] europium,[29] ytterbium,[29−31] and uranium.[32−34] In all of these compounds, the hydrogen atoms bound to the γ-carbon are oriented in such a way as to maximize their distance from the metal atom, in a fashion analogous to that in $(C_5Me_5)La[CH(SiMe_3)_2]_2$ and $(C_5Me_5)Y(OC_6H_3(t\text{-}Bu)_2)[CH(SiMe_3)_2]$. DFT calculations support the idea that there is little if any interaction between the metal and the γ-C−H group and that instead the primary interaction is sigma donation from the Si−C bond.[27,35]

The presence of agostic interactions is best established from structural and spectroscopic data supported by computational studies. Density functional theory (DFT) can make reasonably accurate predictions of the structures of agostic geometries provided that care is taken to choose an appropriate functional.[36−38] Although the classical picture of an agostic interaction involves delocalization of C−H bonding electrons into an empty d-orbital on the metal,[4,8] this simple model has been called into doubt by analysis of the wave functions of agostic complexes.[10,38−40] For example, a computational study of the β-agostic compound $TiCl_3Et(dmpe)$ showed that the β-C−H bonding electrons delocalize principally into orbitals on the α-carbon, rather than into d-orbitals on the metal center.[40] Pantazis et al. extended this concept and suggested that agostic interactions involve delocalization of electrons from the alkyl substituent into an orbital sink, which can be either a vacant d-orbital on the metal, a vacant orbital on the alkyl substituent, or a vacant orbital on another ligand.[38] Computational methods to analyze the interatomic interactions in agostic complexes have recently been reviewed;[10] the natural bond orbital (NBO)[41] and atoms in molecules (AIM)[42] methods are especially useful and widely used. NBO is particularly attractive owing to its implementation in many modern computational chemistry codes and its robustness to the basis sets employed.

Here we describe the new titanium amide complex, $Ti_2Cl_6[N(t\text{-}Bu)_2]_2$, which contains a di(*tert*-butyl)amide ligand that is the carbon analogue of the silylamide ligand $N(SiMe_3)_2$ and structurally similar to the silylalkyl ligand $CH(SiMe_3)_2$. The crystal structure of $Ti_2Cl_6[N(t\text{-}Bu)_2]_2$ reveals that there are short contacts between titanium and a γ-methyl group that are very similar to those seen in the complexes of these isosteric ligands. Such an interaction would normally be expected to be agostic, especially in view of the low formal electron count (12) and low d-electron count (d^0) of the metal center. Despite the presence of these short Ti···H−C contacts, we show here from DFT calculations and other evidence that they are not agostic interactions. In fact, the Ti···H−C interaction is repulsive, and we propose that this situation may be more common than currently realized.

RESULTS AND DISCUSSION

Synthesis and Structure of $Ti_2Cl_6[N(t\text{-}Bu)_2]_2$. Treatment of $TiCl_4$ with two equivalents of $HN(t\text{-}Bu)_2$ in pentane gives an orange solution, from which red crystals of the amido complex $Ti_2Cl_6[N(t\text{-}Bu)_2]_2$ (**1**) can be obtained by crystallization from toluene at −20 °C. The crystals turn green when dried, but redissolve in hydrocarbon solvents to give orange to red solutions. This air- and moisture-sensitive compound can also be obtained in low yield by treatment of $TiCl_4$ with one equivalent of $LiN(t\text{-}Bu)_2$, but this reaction also produces other products.

$$2TiCl_4 + 4HN(t\text{-}Bu)_2 \rightarrow \underset{1}{Ti_2Cl_6[N(t\text{-}Bu)_2]_2} + 2[H_2N(t\text{-}Bu)_2]Cl$$

The room-temperature ^1H and $^{13}C\{^1H\}$ NMR spectra of **1** show a single resonance at δ 1.38 and 32.7, respectively, for the methyl groups of the *tert*-butyl substituents. A discussion of the variable-temperature NMR behavior will be deferred until after presentation of the X-ray crystallographic results.

Single crystals of **1** grown from pentane are polymorphic: the two polymorphs studied, which we will call **A** and **B**, both conform to space group $P2_1/n$. Crystal data for both polymorphs are presented in Table 2. Interestingly, the molecular structures adopted in the two polymorphs are almost exactly identical, and in each polymorph there are two molecules per unit cell, each of which resides on an inversion center. The two polymorphs differ in that the molecules are oriented differently with respect to the screw-axis (Figure 1). The data for polymorph **A** were especially high quality, and selected bond distances and angles for this polymorphs are reported in Table 3.

Compound **1** adopts a dinuclear chloride-bridged structure, in which the $N(t\text{-}Bu)_2$ groups are terminal (Figure 2). The geometry about each titanium atom is distorted square

dx.doi.org/10.1021/om300483v | Organometallics 2012, 31, 4894−4903

Table 2. Crystallographic Data for the Two Polymorphs of $Ti_2Cl_6[N(t\text{-}Bu)_2]_2$

	1A	1B
formula	$C_{16}H_{36}Cl_6N_2Ti_2$	$C_{16}H_{36}Cl_6N_2Ti_2$
fw	564.97	564.97
T (K)	193(2)	193(2)
λ (Å)	0.71073	0.71073
cryst syst	monoclinic	monoclinic
space group	$P2_1/n$	$P2_1/n$
a (Å)	8.5810(16)	7.512(2)
b (Å)	15.042(3)	20.436(7)
c (Å)	10.0622(19)	8.291(3)
β (deg)	91.788(3)	90.484(5)
V (Å^3)	1298.2(4)	1272.8(7)
Z, ρ_{calc} (g cm^{-3})	2, 1.445	2, 1.474
μ (mm^{-1})	1.238	1.262
F(000)	584	584
cryst size (mm)	0.06 × 0.18 × 0.46	0.18 × 0.24 × 0.36
θ range (deg)	2.44−25.37	1.99−28.29
reflns: total/unique	10216/2380	11813/3080
R(int)	0.0495	0.0729
abs corr	face-indexed	face-indexed
max., min. transmn factors	0.931, 0.641	0.808, 0.689
data/restraints/params	2380/12/280	3080/0/126
GOF on F^2	1.005	1.107
R_1 [$I > 2\sigma(I)$]	0.0259	0.0409
wR_2 (all data)	0.0638	0.1153
max., min. $\Delta\rho_{elect}$ (e A^{-3})	0.301, −0.206	0.527, −0.313

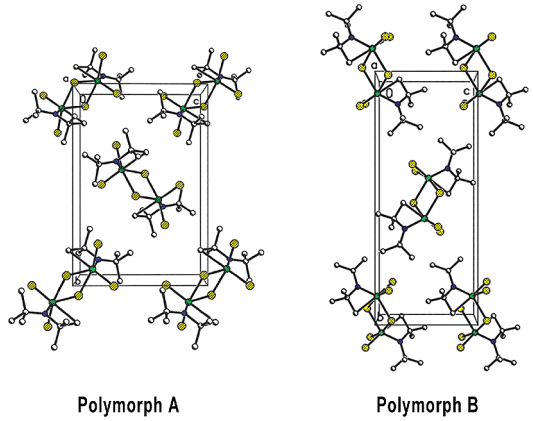

Figure 1. Comparison of molecular packing in the two polymorphs of $Ti_2Cl_6[N(t\text{-}Bu)_2]_2$, both viewed down the a-axis.

pyramidal, with the nitrogen atom, two bridging chlorine atoms, and one terminal chlorine atom making up an equatorial square plane and the remaining terminal chlorine, Cl(1) occupying the axial position. The central Ti_2Cl_2 unit is symmetric about an inversion center with Ti−Cl−Ti angles of 101.96(2)° and Ti−Cl distances to the bridging chlorides of 2.4798(6) and 2.4947(6) Å. The latter are significantly longer than the Ti−Cl distances to the terminal chloride ligands, which are 2.2239(7) and 2.3116(6) Å for the chlorides in the axial and equatorial sites, respectively. The Ti−N distance is 1.871(2) Å.

The most interesting structural feature in **1** is that each titanium center forms a Ti···C close contact of 2.634(3) Å to one of the methyl groups, carbon C(2), of the $N(t\text{-}Bu)_2$ ligand (Figure 2). The presence of the close contact in both polymorphs suggests that this interaction is not the result of packing effects. Including this Ti···C close contact, each titanium atom adopts a distorted octahedral geometry in which the nitrogen atom is trans to one of the bridging chloride atoms, and the Ti···C contact is trans to one of the terminal chloride atoms. Except for the N−Ti···C angle (which is small owing to the fact that these atoms form a four-membered ring), the interligand angles about each Ti center are near the ideal values of 90° and 180°. For comparison, the Ti···C distances in the well-known β-agostic titanium ethyl complex $TiCl_3Et(dmpe)$[43] and in the γ-agostic complex $[Cp_2Ti(C(SiMe_3)=CMePh)][AlCl_4]$[11,12] are 2.501(2) and 2.52 Å, respectively.

All of the hydrogen atoms, including those on the interacting methyl group C(2), were located in the difference map. Interestingly, the hydrogen atoms on C(2) are arranged in a fashion that *maximizes* the distances (and *minimizes* the interaction) between them and the titanium atom. Specifically, one hydrogen atom on C(2) points more or less directly away from the Ti center, and the other two straddle the Ti−C vector. The two shortest Ti···H distances are 2.36(2) and 2.62(2) Å. Interestingly, because the C−H vectors to these two hydrogen atoms are nearly perpendicular to the Ti−H vectors, the Ti−H distances are not greatly affected by the inherent underestimation of C−H distances in X-ray diffraction experiments. If the C−H distance is fixed at 1.08 Å, the recalculated Ti···H distances are 2.35(2) and 2.64(2) Å. For comparison, the shortest Ti···H distances in β-agostic $TiCl_3Et(dmpe)$ and γ-agostic $[Cp_2Ti(C(SiMe_3)=CMePh)][AlCl_4]$ are calculated to be 2.23 and 2.36 Å, respectively.[12] The Ti···C−H angles[44,45] involving the two closest hydrogen atoms in **1** are 95.2° and 80.4°.

The arrangement of hydrogen atoms around C(2) is similar to those seen in certain $CH(SiMe_3)_2$ and $N(SiMe_3)_2$ complexes (see above), in which the metal center is interacting with a C−Si bond. If the interaction in **1** is similar, then we must consider an alternative bonding model, one that involves donation of electron density from the C−C bond of the *tert*-butyl group to the Ti center. If such an interaction is present, then the C(1)−C(2) bond should be elongated. However, no bond lengthening is observed: the C(1)−C(2) bond distance of 1.527(3) Å is essentially identical to the 1.540(3) and 1.529(3) Å bond distances seen between the quaternary carbon and the two noninteracting methyl groups.

A close contact between a metal center and a C−C bond without significant bond lengthening has also been reported in an iridium complex.[46] There are few examples of interactions in which electron density from C−C sigma bonds is suspected to donate to a metal center. In all these cases, either the carbon atoms bear no hydrogen atoms, or the C−H bonds are positioned in such a way that they cannot interact with the metal center.[47−51] For example, lengthening of the C−C bond closest to the metal center has been noted in a niobium cyclopropyl complex,[49,50] and a short Ti−C contact has been observed in a titanium complex of a substituted cyclohexadiene.[47,51] Finally, the structure of a ruthenium quinonoid complex suggests there may be an interaction between the metal center and an aryl−alkyl C−C bond.[48]

Another interesting structural feature of **1** is that the N(1)−C(1)−C(2) angle of 106.65(16)° involving the close-contacting atom C(2) is smaller than the N(1)−C(1)−C(3) and N(1)−C(1)−C(4) angles of 110.3(2)° and 113.22(18)°, respectively, to the other two methyl groups on the quaternary carbon atom C(1) of this *tert*-butyl group. A question here is whether this small angle is due to an agostic interaction between the C(1)−C(2) bond and the Ti center. In fact, there is a more reasonable

dx.doi.org/10.1021/om300483v | *Organometallics* 2012, 31, 4894−4903

Table 3. Selected Bond Lengths and Angles for Polymorph A of $Ti_2Cl_6[N(t\text{-}Bu)_2]_2$, 1a[a]

Bond Distances (Å)					
Ti(1)−N(1)	1.8708(15)	C(2)−H(2A)	0.99(2)	C(5)−C(8)	1.534(3)
Ti(1)−Cl(1)	2.2239(7)	C(2)−H(2B)	0.91(3)	C(6)−H(6A)	0.98(3)
Ti(1)−Cl(2)	2.3116(6)	C(2)−H(2C)	0.96(2)	C(6)−H(6B)	0.94(3)
Ti(1)−Cl(3)	2.4798(6)	C(3)−H(3A)	0.99(2)	C(6)−H(6C)	0.95(4)
Ti(1)−Cl(3′)	2.4947(6)	C(3)−H(3B)	0.87(3)	C(7)−H(7A)	0.92(3)
Ti(1)−C(2)	2.634(3)	C(3)−H(3C)	0.97(2)	C(7)−H(7B)	1.01(3)
N(1)−C(1)	1.511(2)	C(4)−H(4A)	0.90(3)	C(7)−H(7C)	1.00(3)
N(1)−C(5)	1.518(2)	C(4)−H(4B)	0.96(3)	C(8)−H(8A)	1.05(3)
C(1)−C(2)	1.527(3)	C(4)−H(4C)	0.99(3)	C(8)−H(8B)	1.00(2)
C(1)−C(3)	1.540(3)	C(5)−C(6)	1.524(4)	C(8)−H(8C)	0.94(3)
C(1)−C(4)	1.529(3)	C(5)−C(7)	1.532(4)		
Bond Angles (deg)					
Ti(1)−N(1)−C(1)	110.66(11)		Cl(3′)−Ti(1)−C(2)	82.34(6)	
Ti(1)−N(1)−C(5)	125.44(12)		N(1)−Ti(1)−C(2)	62.84(7)	
Cl(1)−Ti(1)−N(1)	114.30(5)		N(1)−C(1)−C(2)	106.65(16)	
Cl(1)−Ti(1)−Cl(2)	94.65(3)		N(1)−C(1)−C(3)	110.3(2)	
Cl(1)−Ti(1)−Cl(3)	91.53(2)		N(1)−C(1)−C(4)	113.22(18)	
Cl(1)−Ti(1)−Cl(3′)	100.22 (2)		N(1)−C(5)−C(6)	116.4(2)	
Cl(1)−Ti(1)−C(2)	176.46(6)		N(1)−C(5)−C(7)	107.57(19)	
Cl(2)−Ti(1)−N(1)	98.88 (5)		N(1)−C(5)−C(8)	108.46(18)	
Cl(2)−Ti(1)−Cl(3)	163.09(2)		C(1)−N(1)−C(5)	123.73(14)	
Cl(2)−Ti(1)−Cl(3′)	85.37(2)		H(2A)−C(2)−H(2B)	109.2(17)	
Cl(2)−Ti(1)−C(2)	87.97(7)		H(2A)−C(2)−H(2C)	112.1(17)	
Cl(3)−Ti(1)−N(1)	92.86(5)		H(2B)−C(2)−H(2C)	104.5(19)	
Cl(3)−Ti(1)−Cl(3′)	78.044(19)		C(2)−C(1)−C(3)	107.7(2)	
Cl(3)−Ti(1)−C(2)	86.60(7)		C(2)−C(1)−C(4)	106.7(2)	
Cl(3′)−Ti(1)−N(1)	144.59(5)		C(3)−C(1)−C(4)	111.9(2)	

[a]The symbol ′ denotes inversion-related atoms.

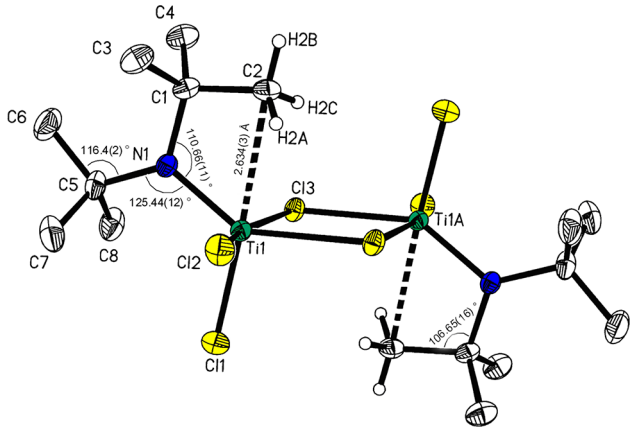

Figure 2. X-ray crystal structure of $Ti_2Cl_6[N(t\text{-}Bu)_2]_2$, **1**. Ellipsoids are drawn at the 30% probability density level, except for hydrogen atoms, which are shown as arbitrarily sized spheres.

explanation: the closing of the N(1)−C(1)−C(2) angle is almost certainly due to steric repulsions between the two bulky *tert*-butyl groups attached to nitrogen. The most convincing evidence of this effect is that the N(1)−C(5)−C(6) angle to the methyl group on the remote *tert*-butyl substituent is significantly opened up (Figure 2). This methyl group is closest to the *tert*-butyl substituent involved in the close interaction. In short, both distortions are entirely consistent with tilting of the *tert*-butyl groups away from one another to reduce steric repulsions between them.

Variable-Temperature NMR Behavior of $Ti_2Cl_6[N(t\text{-}Bu)_2]_2$. At room temperature the ^{1}H NMR spectrum of **1** in toluene-d_8 shows a sharp singlet for the *tert*-butyl groups at δ 1.38. When the sample is cooled, the peak begins to broaden, but is still a broad singlet at −60 °C. At −90 °C the broad resonance has decoalesced into three singlets, which sharpen upon further cooling to −100 °C. At the latter temperature, the three resonances at δ 1.40, 0.87, and 0.62 have relative intensities of 12:3:3, respectively. The spectra suggest that rotation about the Ti−N bond, as well as about one of the N−C bonds, becomes slow on the NMR time scale at low temperatures. Such a situation should give a spectrum containing four resonances with intensities of 9:3:3:3, corresponding to one *tert*-butyl group and three methyl groups. Evidently, the resonance for one of the methyl groups overlaps with the resonance for the *tert*-butyl group to give the observed 12:3:3 intensity pattern. The spectra are equally consistent with slowing of rotation of the *tert*-butyl group that is interacting with the metal center, as well as the remote *tert*-butyl group that is near the axial atom Cl(1).

Owing to the overlap of some of the resonances and because at least two exchange processes are operating in **1** (rotation about the N−C bonds and rotation about the Ti−N bonds), we did not attempt to obtain barriers for these two dynamic processes from fits to the line shapes. We could estimate from the general decoalescence behavior, however, that both barriers must be about 10 ± 2 kcal/mol. Finally, we point out that the NMR data are consistent with the structure of **1** as deduced crystallographically, although they do not rule out the possibility that **1** is a monomer in solution.

DFT Structures of $Ti_2Cl_6[N(t\text{-}Bu)_2]_2$. In order to probe the nature of the close interactions in **1**, gas-phase structures were optimized using three different DFT functionals: B3LYP, M05-2X, and PBE0. The calculated structure is shown in Figure 3. All

dx.doi.org/10.1021/om300483v | *Organometallics* 2012, 31, 4894−4903

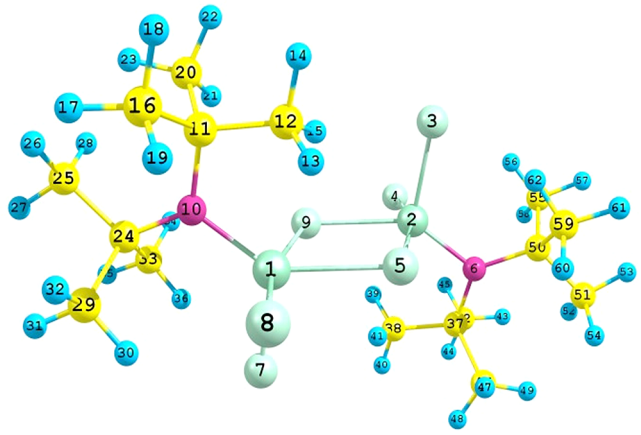

Figure 3. Structure of $Ti_2Cl_6[N(t\text{-}Bu)_2]_2$ from PBE0 calculations.

functionals afforded optimized structures whose interatomic distances (Table 4) agreed within 0.1 Å of those seen for the crystal structure, except for the carbon−hydrogen distances, which as usual are systematically underestimated by ∼0.15 Å by X-ray diffraction.[52] Specifically, the calculated structure contains the same short Ti1···C12 contact with one of the ligand methyl groups found experimentally. The calculated distances (Å) for this contact are 2.767 (B3LYP), 2.688 (PBE0), and 2.662 (M05-2X), versus the experimental value of 2.634(2). These comparisons suggest that M05-2X and PBE0 do a better job than B3LYP in modeling weak M···H−C interactions, a conclusion we have also reached in a benchmark study of a different system.[37] From here on, we will focus our discussion on the PBE0 calculations; results from M05-2X and B3LYP can be found in Table 4 and in the Supporting Information.

In the calculated structure, the hydrogen atoms attached to the methyl group involved in the close contact are disposed in such a way as to maximize the Ti···H distances, exactly as seen crystallographically. For PBE0, the shortest and second shortest Ti1···H distances of 2.46 and 2.68 Å agree well with the experimental values of 2.36(2) and 2.62(2) Å. The structural similarities between these gas-phase models and the crystal structure suggest that the close Ti···H−C contacts seen in the crystal structure are not significantly influenced by packing effects.

Although such short Ti···H distances are often indicative of agostic interactions,[2] other calculated structural features are less consistent with this interpretation. The calculated C−H bond closest to the Ti center is only 0.002 Å longer than the other C−H bonds in the molecule, whereas C−H bond lengthenings of 0.04 Å are typical for M···H−C interactions in other transition metal complexes.[10,36] Similarly, the C−C bond closest to the titanium (C11−C12) is only 0.004 to 0.006 Å longer than the two other C−C bonds in the same *tert*-butyl substituent (C11−C16 and C11−C20). Thus, the calculations show little evidence of significant weakening of the C−H bond or distortion of the alkyl substituent due to a Ti···H−C or Ti···C interaction.

Kohn−Sham and NBO Analysis of 1. Kohn−Sham orbitals were calculated for **1** from the results of the DFT calculations with PBE0. The HOMO (Figure 4a) is predominantly a π-bond between a titanium d-orbital and the "lone pair" p-orbital on the amide nitrogen, along with a small amount of titanium−chlorine antibonding. Even at relatively inclusive electron density contour values of 0.02 e $Å^{-3}$, the HOMO clearly shows no overlap between the titanium and the γ-carbon. An examination of all occupied Kohn−Sham orbitals revealed none with a significant interaction between the titanium center and the carbon or hydrogen atoms of the *tert*-butyl group engaged in the close contact. In contrast, the Kohn−Sham orbitals of the classical beta-agostic complex, $TiEtCl_3(dmpe)$ (Figure 4b), show clear orbital overlap between the Ti and beta-agostic C−H bond.[53]

The natural bond orbital method has been used to test for the presence of agostic interactions in other systems,[36,54] and we find these methods useful here. In NBO, the many-electron wave function is analyzed in terms of electron-pair bonding units within an idealized Lewis structure.[41,55] In structures with delocalized electrons, perturbation theory is used to calculate donor−acceptor interactions between occupied Lewis pair orbitals and unoccupied orbitals. The larger the stabilization energy due to the donor−acceptor interaction, the more stable the bond. The limit of this donor−acceptor interaction is a hypervalent three-center−two-electron bond.

One would expect a strong agostic interaction to exhibit this kind of three-center delocalization. We find that, for all three DFT methods, there are no three-center bonds between the titanium atom and any C−H or C−C bond in **1**. However, a weak donor−acceptor interaction between the C−H bonding orbital closest to the Ti center and an empty Ti d-orbital can be

Table 4. Geometrical Parameters for $Ti_2Cl_6[N(t\text{-}Bu)_2]_2$, 1, from DFT and from the X-ray Crystal Structure[a]

parameter	B3LYP	PBE0	M05-2X	X-ray structure	expt
Ti1···H13	**2.515**	**2.463**	**2.453**	**Ti(1)−H(2A)**	**2.36(2)**
Ti1···H15	**2.774**	**2.677**	**2.678**	**Ti(1)−H(2C)**	**2.62(2)**
Ti1···C12	**2.767**	**2.688**	**2.662**	**Ti(1)−C(2)**	**2.634(2)**
C12−H13	1.095	1.098	1.094	C(2)−H(2A)	0.98(2)
C12−H14	1.093	1.093	1.090	C(2)−H(2B)	0.91(3)
C12−H15	1.093	1.095	1.092	C(2)−H(2C)	0.96(2)
C11−C12	1.549	1.540	1.545	C(1)−C(2)	1.527(3)
C11−C16	1.544	1.534	1.534	C(1)−C(3)	1.540(3)
C11−C20	1.546	1.536	1.537	C(1)−C(4)	1.528(3)
Ti1−N10−C11	113.6	112.4	111.0	Ti(1)−N(1)−C(1)	110.7(1)
N10−C11−C12	108.1	107.4	108.3	N(1)−C(1)−C(2)	106.65(16)
N12−C11−C16	110.6	110.7	110.7	N(1)−C(1)−C(3)	110.3(2)
N12−C11−C20	112.7	112.8	112.0	N(1)−C(1)−C(4)	113.22(18)
Ti1···H13−C12	**65.3**	**89.5**	**67.1**	**Ti(1)−H(2A)−C(2)**	**95.29(7)**

[a]Parameters in bold relate directly to the Ti···H−C close contact. Distances in Å and angles in degrees.

dx.doi.org/10.1021/om300483v | *Organometallics* 2012, 31, 4894−4903

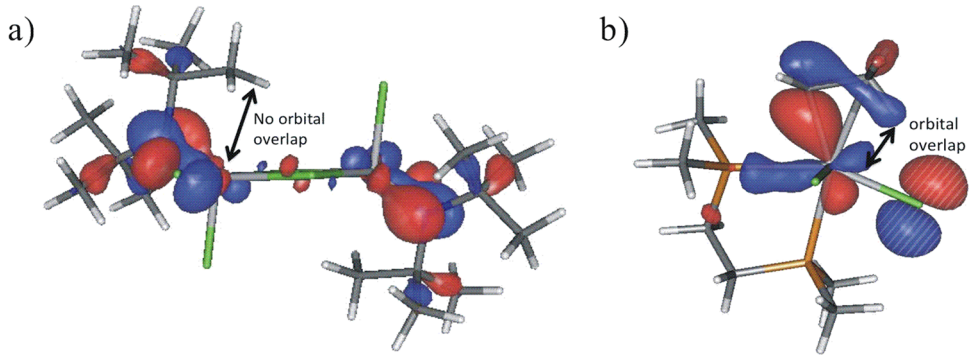

Figure 4. HOMO of (a) $Ti_2Cl_6[N(t\text{-}Bu)_2]_2$, **1**, and (b) $TiCl_3Et(dmpe)$ as determined by PBE0. The surface contours represent electron densities of 0.05 e $Å^{-3}$.

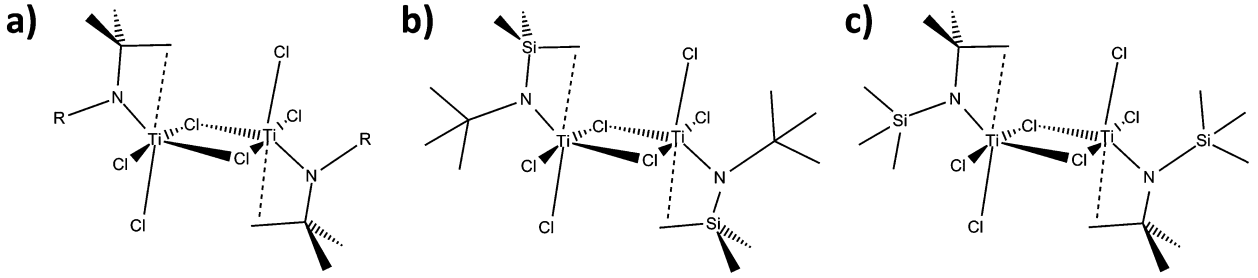

Figure 5. Schematic illustration of structures used in the DFT calculations: (a) $Ti_2Cl_6[NR(t\text{-}Bu)]_2$, where R = Me, Et, $SiMe_3$, or *t*-Bu, and two rotameric conformers of $Ti_2Cl_6[N(t\text{-}Bu)(SiMe_3)]_2$, where the $SiMe_3$ group is oriented (b) nearest the Ti atom or (c) remote from the Ti atom.

found. This interaction results in a stabilization of 2.1 kcal mol^{-1} (PBE0). For comparison, DFT calculations on a niobium complex using the PBE0 functional found that a *β*-agostic interaction afforded a stabilization energy of 23.8 kcal mol^{-1}, whereas a similar nonbonded (i.e., nonagostic) interaction involving the same orbitals had a stabilization energy of only 1.7 kcal mol^{-1}.[36] Accordingly, the stabilization afforded by the donor−acceptor interaction in the present complex **1** is characteristic of that of a nonbonded interaction rather than of an agostic interaction.

Steric Effects as the Cause of the Close Contact in 1. As judged from the theoretical treatments and detailed structural comparisons, the close Ti···H and Ti···C contacts in **1** are best thought of as nonbonding. We will show in this section that they are the result of minimization of interligand steric interactions: specifically, avoidance of unfavorable contacts between chlorine atom Cl(1) and the amido *tert*-butyl group that is not involved in the close contact with the metal center. Evidence in support of this conclusion is the presence of a short nonbonded contact of 3.48 Å between chlorine atom Cl(1) and carbon atom C(8), one of the methyl carbons of the *tert*-butyl group that is not involved in the close contact (which we will call the remote *tert*-butyl group). For comparison, the van der Waals radii of Cl and CH_3 are 1.75 and 2.0 Å, respectively, so that the Cl(1)−C(8) distance is more than 0.25 Å shorter than the sum. In order to avoid making this contact distance even shorter, the Cl(1)−Ti(1)−N(1) angle of 114.30(5)° is quite large, and the substituents on the amide nitrogen atom are pivoted away from Cl(1) so that the two Ti−N−C angles are different by 15°: the Ti−N−C angle to the *tert*-butyl group closest to Cl(1) is 125.4°, whereas the angle to the *tert*-butyl group farthest from Cl(1) is 110.6°. The net effect is to move the amide group away from Cl(1) and place the *tert*-butyl group farthest from Cl(1) close to the titanium center.

Thus, interligand steric congestion appears to be the key factor that forces one *tert*-butyl C−H bond into close interaction with the titanium atom. If this explanation is correct, then replacing the remote *tert*-butyl group on the amide ligand with smaller substituents should allow the *tert*-butyl group nearest the titanium center to move farther away from the metal. We therefore calculated gas-phase structures for $Ti_2Cl_6[NR(t\text{-}Bu)]_2$ molecules in which the remote substituent R on the amido ligand is Me, Et, or $SiMe_3$ (Figure 5a). Relative to **1**, the methyl and ethyl analogues will be much less sterically crowded, whereas the $SiMe_3$ analogue will be slightly less crowded. Important geometric parameters for these molecules are shown in Table 5.

Table 5. Geometric Parameters (PBE0 functional) for $Ti_2Cl_6[NR(t\text{-}Bu)]_2$ with Different Remote Substituents R on the Amido Ligand

parameter	R = Me	R = Et	R = $SiMe_3$	R = *t*-Bu
Ti···H[a] (Å)	2.72	2.81	2.60	2.46
Ti···C[b] (Å)	2.94	3.08	2.79	2.68
Ti−N−X[c] (deg)	121.8	125.6	116.5	112.4

[a]H closest to titanium center. [b]C closest to titanium center. [c]X = Si or C.

One of these molecules, $Ti_2Cl_6[N(SiMe_3)(t\text{-}Bu)]_2$, has been studied crystallographically:[56] this molecule adopts a structure that is very similar to that of **1**. Specifically, the *tert*-butyl group in this complex forms a Ti···C contact of 2.774 Å, which is longer than the Ti···C contact of 2.634(2) Å in **1**. As seen in **1**, the hydrogen atoms on the *tert*-butyl groups of $Ti_2Cl_6[N(SiMe_3)(t\text{-}Bu)]_2$ are oriented so as to minimize their interactions with the Ti atom. The other experimental parameters for this complex are very similar to those seen for **1**: for example, the Ti−N distance is 1.838(2) versus 1.871(2) Å in **1**. The optimized DFT structure

dx.doi.org/10.1021/om300483v | *Organometallics* 2012, 31, 4894−4903

for the $SiMe_3$ analogue exhibits similar parameters: the calculated Ti···C close contact is 2.79 Å, the Ti−N distance is 1.82 Å, and the shortest Ti···H distances are 2.60 and 2.74 Å.

Relative to carbon−carbon bonds, silicon−carbon bonds are longer and have higher energy sigma bonding orbitals; therefore a Si−C bond is a better donor than a C−C bond. If the driver for forming a close interaction between the Ti center and a substituent on the amide group is reducing the electron-deficient nature of the titanium center, then we would expect that the $SiMe_3$ group should be the substituent that interacts with the titanium center in $Ti_2Cl_6[N(t\text{-Bu})(SiMe_3)]_2$. This is not the structure observed experimentally, however: the *tert*-butyl group is closes to Ti center. To obtain more information about this point, we carried out energy calculations on two different rotamers of this $N(t\text{-Bu})(SiMe_3)$ compound: one in which the $SiMe_3$ group is closest to Ti (Figure 5b) and one in which the *tert*-butyl group is closest to Ti (as observed experimentally; Figure 5c). We found that the latter rotamer is in fact lower in energy by 3.30 kcal mol^{-1}.

Thus, in both the experimental and calculated structures, the *tert*-butyl group is engaged in the close interaction with the Ti center. The $SiMe_3$ group takes the remote position, where it is located near an axial chlorine atom. This overall molecular geometry is consistent with minimization of steric repulsions between the amido ligand and the chlorine atoms. By placing the *tert*-butyl group near the titanium and the $SiMe_3$ group near the axial chlorine, the steric interactions with those chlorine atoms are reduced. A similar minimization of steric effects can account for the structure of **1**.

We also optimized the structures of analogues of **1** in which the remote substituent is a methyl or ethyl group. Owing to the much smaller steric sizes of these substituents, interligand steric interactions between the two substituents on nitrogen, and interligand steric interactions with the chlorine atom Cl(1) are much reduced. As a result, the *tert*-butyl group is able to move away from the titanium center (Figure 6). Thus, the calculated

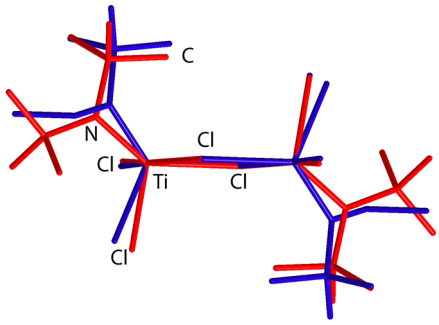

Figure 6. Superposition of PBE0-calculated structures of $Ti_2Cl_6[N(t\text{-Bu})_2]_2$, **1** (red), and $Ti_2Cl_6[NEt(t\text{-Bu})]_2$ (blue), which have different substituents R in the remote site on the amide ligand. The calculated distances for the close Ti−H interaction in these structures are 2.46 Å for R = *t*-Bu and 2.81 Å for R = Et.

Ti−H distance increases from 2.46 Å for R = *t*-Bu, to 2.60 Å for R = $SiMe_3$, to 2.81 Å for R = Et, and to 2.72 Å for R = Me. Similarly, the calculated Ti−N−C angles involving the *tert*-butyl group closest to the metal center (which are a measure of how much the steric interactions force the *tert*-butyl group to interact with the Ti center) are 112.4°, 116.5°, 125.6°, and 121.8° for R = *t*-Bu, $SiMe_3$, Et, and Me, respectively. These angles increase as the remote substituent becomes smaller, thus enabling the *tert*-butyl group to move away from the titanium center.

The geometries of the R = Et and Me complexes do not follow exactly the trend expected from the relative sizes of these two groups. This appears to be a real effect because, as far as we can tell, both structures are global rather than local minima. The methyl-substituted amide (but not the ethyl analogue) adopts a rotational conformation for the methyl group in which one hydrogen points toward the terminal chloride ligand; therefore the geometry methyl analogue has a slightly greater repulsive interaction between the Me group on nitrogen and the terminal chlorine atom. Presumably, this energy penalty is compensated by reduced repulsive interactions elsewhere in the molecule, but we have not explored this point in detail.

Wiberg bond overlap indices can provide useful information about the nature of the Ti···H interactions in these molecules (Table 6). As a benchmark, the bond overlap indices for the *β*-

Table 6. Wiberg Bond Overlap Indices Calculated by PBE0 for Key Bonds in $Ti_2Cl_6[NR(t\text{-Bu})]_2$ where R = Me, Et, $SiMe_3$, or *t*-Bu[a]

parameter	R = Me	R = Et	R = $SiMe_3$	R = *t*-Bu
Ti1···Ti2	0.05	0.05	0.05	0.05
Ti1−Cl5	0.81	0.82	0.76	0.75
Ti1−Cl7	1.48	1.44	1.47	1.47
Ti1−Cl8	1.30	1.34	1.37	1.29
Ti1−Cl9	0.61	0.58	0.65	0.68
Ti1−N10	1.28	1.29	1.37	1.29
Ti1···C11	0.03	0.03	0.04	0.04
Ti1···C12	**0.01**	**0.01**	**0.09**	**0.12**
Ti1···H13	**0.02**	**0.02**	**0.04**	**0.04**
Ti1···H14	0.00	0.00	0.00	0.01
Ti1···H15	0.02	0.01	0.02	0.03
C11−C12	0.99	0.99	0.99	0.98
C11−C16	0.99	0.99	0.99	0.99
C11−C20	0.99	0.99	0.99	0.99
C12−H13	**0.88**	**0.89**	**0.87**	**0.85**
C12−H14	**0.90**	**0.90**	**0.89**	**0.88**
C12−H15	0.88	0.91	0.88	0.86
C16−H17	0.91	0.92	0.92	0.92
C16−H18	0.91	0.91	0.91	0.91
C16−H19	0.91	0.92	0.91	0.90

[a]The numbers in bold are discussed in the text.

agostic complex $TiEtCl_3(dmpe)$ are 0.17 and 0.11 for Ti···C_β and Ti···H, respectively. In contrast, the overlap indices for *t*-Bu complex **1** are significantly smaller: 0.12 for the Ti1···C12 interaction and 0.04 for the Ti1···H13 interaction. The bond overlap indices decrease even further as the interligand steric repulsions involving the remote substituent decrease and interactions with the Ti center become longer: the Ti···C bond index decreases from 0.09 ($SiMe_3$) to 0.01 (Et) to 0.01 (Me), and the Ti···H bond index decreases in the same manner from 0.04 ($SiMe_3$) to 0.02 (Et) to 0.02 (Me). The results above show clearly that, as the remote interligand repulsions decrease, the Ti···C and Ti···H close contacts to the *tert*-butyl group lengthen, and the corresponding bond overlap indices diminish.

Thus, we conclude that the close Ti···H interaction in **1** is a result of the steric repulsions between the two substituents on nitrogen, and between the remote substituent on the amide and one of the terminal chloride ligands. These interactions cause a distortion in the amide ligand that forces a methyl group of one of the *tert*-butyl substituents to lie close to the Ti center. Interestingly, the bond overlap indices for all three C−H

dx.doi.org/10.1021/om300483v | *Organometallics* 2012, 31, 4894−4903

bonds of this methyl group are only 0.85−0.88, versus 0.91−0.92 for the C−H bonds of the other two methyl groups on the *tert*-butyl substituent. The reduction in the C−H bond overlap indices for the methyl group involved in the close contact may actually be due to the destabilization of these bonds as a result of the nonbonding interactions with the titanium center.

Other aspects of the Wiberg bond index analysis are as expected. There is considerable π-donation from the amide nitrogen, as shown by the Ti−N bond index of 1.47, and from the terminal chlorides, as shown by the Ti−Cl bond overlap indices of 1.47 (trans to the nonagostic interaction) and 1.29 (trans to a bridging chloride). The bond overlap indices to the bridging chlorides are 0.68 and 0.75.

We believe that the donor properties of the amide and chloride ligands are responsible for the fact that the close interactions to the γ-methyl group in **1** are repulsive rather than attractive. In general, strong σ-donors will raise the energies of the d-orbitals by shielding effects, and strong π-donors will raise the energies of the d-orbitals by mixing with them. In both cases, raising the energies of the empty d-orbitals on the metal center will make them less suited for engaging in agostic interactions. In **1**, the γ-methyl interaction is almost exactly trans to a terminal chloride ligand that that is acting as a π-donor. The γ-methyl interaction is also cis to a very strongly σ- and π-donating amide ligand and to one terminal and two bridging chloride ligands, all three of which are weak π-donors (even though the π-bond order is high, the chlorides are too electronegative to be strong π-donors). As a result of these σ- and π-donor interactions, the d-orbital(s) that are "pointing" toward the γ-methyl group in **1** will be relatively high in energy. In contrast, the β-carbon of the ethyl group in $TiEtCl_3(dmpe)$ is located trans to a non-π-donor ligand and cis to another (the phosphorus atoms of the chelating phosphine). Even though three weakly π-donating chloride ligands are present, the net donor effect of the ligand set leaves the energies of some of the d-orbitals relatively low, and therefore the β-carbon of the ethyl group can form a true agostic interaction.

Concluding Remarks. The titanium amide $Ti_2Cl_6[N(t\text{-}Bu)_2]_2$, **1**, exhibits a close Ti···C contact of 2.634(3) Å between each titanium center and one of the γ-carbon atoms in the *tert*-butyl groups of the bound amido ligand. In addition, there is a short Ti···H contact of 2.36(2) Å that is well within the range characteristic of agostic interactions. However, the rotational orientation of the methyl group (which maximizes rather than minimizes the Ti···H distances) suggests that the Ti···H interactions are repulsive. DFT calculations support this conclusion: overlap between the Ti d-orbitals and C−H orbitals is small, and there is no evidence of significant weakening of the C−H (or C−C) bond nearest the Ti center in **1**. These and other results strongly suggest that what appears from structural data to be a γ-agostic interaction is actually a result of intraligand and interligand steric repulsions between the remote *tert*-butyl group on the amide and one of the terminal chloride ligands. These results constitute a very nice illustration of a statement by Maseras and Crabtree, who pointed out that a close contact between a metal and a X−Y bond can be classified as agostic only if two conditions are fulfilled: (i) there must be an empty orbital capable of overlap with the bond in question, and (ii) there must also be some evidence of weakening of the bond.[46] We point out that the latter feature is often most readily accessible by calculation.

Steric effects have previously been discussed in the context of agostic interactions,[50,57−59] but the present complex provides an unusually clear example of the ability of steric interactions to generate what is apparently (but is not) a significant agostic interaction. An important conclusion is that close M···H−C contacts observed structurally may actually be repulsive rather than attractive. Such behavior seems to be especially likely for compounds that contain close contacts with γ-carbons,[10,25,27,60] but is certain to be present in many other kinds of compounds as well. Such repulsive interactions are likely to be found in complexes that possess strong σ- or π-donors in the coordination sphere of the metal atom (such as an amido ligand), which will raise the energies of the empty d-orbitals.

EXPERIMENTAL SECTION

All operations were carried out in a vacuum or under argon with standard Schlenk techniques. All glassware was flame-dried before use. Pentane was distilled under nitrogen from sodium benzophenone, and the $TiCl_4$ (Strem) was distilled before use. The reagents $HN(t\text{-}Bu)_2$ and $LiN(t\text{-}Bu)_2$ were prepared by a modification of a literature route.[61]

Elemental analyses were performed by the University of Illinois Microanalytical Laboratory. The IR spectra were obtained on a Nicolet Impact 410 spectrometer as Nujol mulls between KBr plates. The ^1H and ^{13}C NMR data were recorded on a Varian Unity-500 spectrometer at 11.75 T. Chemical shifts are reported in δ units (positive shifts to higher frequency) relative to TMS. X-ray crystallographic data were collected at the University of Illinois Materials Chemistry Laboratory.

Hexachlorobis[di(*tert*-butyl)amido]dititanium(IV). To a stirred solution of $HN(t\text{-}Bu)_2$ (1.04 mL, 6.08 mmol) in pentane (50.0 mL) at 25 °C was added titanium(IV) chloride (0.33 mL, 3.01 mmol). The mixture was stirred for 18 h, and then the solvent was removed under vacuum; the solid was extracted with pentane (5 × 30 mL). The extracts were cooled to −20 °C, without concentrating, for 16 h to afford the product as green needles. Polymorphs A and B are obtained under seemingly identical conditions. Yield: 0.10 g (11.8%). Anal. Calcd for $C_{16}H_{36}Cl_6N_2Ti_2$: C, 34.0; H, 6.42, N, 4.96, Cl, 37.6. Found: C, 34.1, H, 6.80, N, 4.98, Cl, 36.9. ^1H NMR (C_7D_8, 25 °C): δ 1.38 (s, *t*-Bu). ^{13}C NMR (C_7H_8, 25 °C): δ 32.7 (s, *t*-Bu). IR (cm^{-1}): 1243 (m), 1209 (m), 1178 (br, m), 1044 (w), 931 (w), 901 (w), 846 (m), 802 (w), 758 (w), 575 (m), 444 (m).

Crystallographic Studies (ref 62). Single crystals of $Ti_2Cl_6[N(t\text{-}Bu)_2]_2$ polymorph A (**1a**), grown from pentane, were mounted on glass fibers with Paratone-N oil (Exxon) and immediately cooled to −75 °C in a cold nitrogen gas stream on the diffractometer. Crystals of $Ti_2Cl_6[N(t\text{-}Bu)_2]_2$ polymorph B (**1b**) were obtained and treated similarly [subsequent comments in brackets will refer to this compound]. Standard peak search and indexing procedures gave rough cell dimensions, and least-squares refinement using 995 [934] reflections yielded the cell dimensions given in Table 2. Data were collected with an area detector by using the measurement parameters listed in Table 2. The measured intensities were reduced to structure factor amplitudes and their estimated standard deviations by correction for background, scan speed, and Lorentz and polarization effects. Corrections for crystal decay were unnecessary. Systematically absent reflections were deleted and symmetry equivalent reflections were averaged to yield the set of unique data. For all three structures, systematic absences for $0k0$ ($k \neq 2n$) and $h0l$ ($h + l \neq 2n$) were consistent only with space group $P2_1/n$. A face-indexed absorption correction was applied, the maximum and minimum transmission factors being 0.931 and 0.641. [For **1b**, no absorption correction was applied.] All 2380 [3080] data were used in the least-squares refinement. The structures were solved using direct methods (SHELXTL). The analytical approximations to the scattering factors were used, and all structure factors were corrected for both real and imaginary components of anomalous dispersion. The quantity minimized by the least-squares program was $\sum w(F_o^2 - F_c^2)^2$, where $w = \{[\sigma(F_o^2)]^2 + (0.039P)^2\}^{-1}$ and $P = (F_o^2 + 2F_c^2)/3$. [For **1b**, $w = \{[\sigma(F_o^2)]^2 + (0.0493P)^2 + 1.06P\}^{-1}$.] In the final cycle of least-squares, independent anisotropic displacement factors were refined for all atoms, including the hydrogen atoms, all of which appeared as distinct peaks in the difference maps and whose locations were refined without restraints. [For **1b**, the data crystal was twinned by merohedry; the calculated

dx.doi.org/10.1021/om300483v | *Organometallics* 2012, 31, 4894−4903

intensities were defined by the formula $I_{calc} = xI(hkl) + (1 - x)I(\bar{h}\bar{k}\bar{l})$, where x is the volume fraction of the major twin individual. The value of x refined to 0.898(1). In the final cycle of least-squares, independent anisotropic displacement factors were refined for all non-hydrogen atoms, and the hydrogen atoms were fixed in "idealized" positions with their isotropic displacement parameters set equal to 1.5 times U_{eq} for the attached carbon atom.] Successful convergence was indicated by the maximum shift/error of 0.001 for the last cycle. The largest peak in the final Fourier difference map (0.30 e Å^{-3}) was located 0.72 Å from N1 and 1.27 Å from Ti1. [For **1b**, the largest peak in the final Fourier difference map (0.53 e Å^{-3}) was located 0.91 Å from N1 and 1.03 Å from Ti1.] Final refinement parameters are given in Table 2. A final analysis of variance between observed and calculated structure factors showed no apparent errors.

Computational Methods. All gas-phase structures were optimized in C_i (inversion) symmetry using Gaussian03 Rev. E.01.[63] Pople's 6-31G(d,p) basis set[64] was used for the C and H atoms, and Pople's 6-31G basis set[64] was used for the N atoms. To reduce the time required for the calculations, lanl2 effective core potentials[65,66] were used on the Cl and Ti atoms. The lanl2dz basis set was used for Ti. Electron affinity calculations (see Supporting Information) showed that polarization functions were required to describe accurately chlorine atoms, and therefore lanl2dz(d,p)[67] was used for chlorine. The crystal structure of **1** was used as a starting point for all geometry optimizations carried out with the functionals B3LYP,[68,69] PBE0 (also known as PBE1PBE),[70] and M05-2X.[71] Stationary points were verified to be local minima in two ways: all vibrational frequencies were non-negative, and the same structure resulted upon reoptimization after a manual distortion, such as changing the N10−C11−C12−H13 dihedral angle or the Ti1−N10−C11 angle to a value different from that in the optimized structure. Natural bond orbitals were calculated from the optimized structures for each of the complexes using NBO 3.0 as implemented in Gaussian03.

■ ASSOCIATED CONTENT

Supporting Information

Electron affinities for chlorine calculated for basis sets and functionals used in this study. Table correlating atomic labels in the crystal structure of **1** and the theoretical model. Optimized structures from calculations on $Ti_2Cl_6[NR(t\text{-}Bu)]_2$, where R is *t*-Bu (**1**), $SiMe_3$, Et, or Me. This material is available free of charge via the Internet at http://pubs.acs.org.

■ AUTHOR INFORMATION

Notes

The authors declare no competing financial interest.

■ ACKNOWLEDGMENTS

The authors thank the National Science Foundation for support under grant CHE 11-12360, and Scott Wilson and Teresa Prussak-Wieckowska for collecting the single-crystal X-ray diffraction data. This research was supported in part by the National Science Foundation through TeraGrid resources provided by the National Center for Supercomputing Applications.

■ REFERENCES

(1) Brookhart, M.; Green, M. L. H. *J. Organomet. Chem.* **1983**, *250*, 395−408.
(2) Brookhart, M.; Green, M. L. H.; Parkin, G. *Proc. Natl. Acad. Sci. U. S. A.* **2007**, *104*, 6908−6914.
(3) Brookhart, M.; Green, M. L. H.; Wong, L. L. *Prog. Inorg. Chem.* **1988**, *36*, 1−124.
(4) Clot, E.; Eisenstein, O. *Struct. Bonding (Berlin)* **2004**, *113*, 1−36.
(5) Kubas, G. J., Ed. *Metal Dihydrogen and σ-Bond Complexes: Structure, Theory and Reactivity*; Kluwer: Dordrecht, 2001.
(6) Scherer, W.; McGrady, G. S. *Angew. Chem., Int. Ed.* **2004**, *43*, 1782−1806.
(7) Goddard, R. J.; Hoffmann, R.; Jemmis, E. D. *J. Am. Chem. Soc.* **1980**, *102*, 7667−7676.
(8) Eisenstein, O.; Jean, Y. *J. Am. Chem. Soc.* **1985**, *107*, 1177−1186.
(9) Vidal, I.; Melchor, S.; Alkorta, I.; Elguero, J.; Sundberg, M. R.; Dobado, J. A. *Organometallics* **2006**, *25*, 5638−5647.
(10) Lein, M. *Coord. Chem. Rev.* **2009**, *253*, 625−634.
(11) Eisch, J. J.; Piotrowski, A. M.; Brownstein, S. K.; Gabe, E. J.; Lee, F. L. *J. Am. Chem. Soc.* **1985**, *107*, 7219−7221.
(12) Koga, N.; Morokuma, K. *J. Am. Chem. Soc.* **1988**, *110*, 108−112.
(13) Wong, W. K.; Jiang, T.; Wong, W. T. *J. Chem. Soc., Dalton Trans.* **1995**, 3087−3088.
(14) Gillett-Kunnath, M.; Teng, W. J.; Vargas, W.; Ruhlandt-Senge, K. *Inorg. Chem.* **2005**, *44*, 4862−4870.
(15) Goldfuss, B.; Schleyer, P. V.; Handschuh, S.; Hampel, F. *J. Organomet. Chem.* **1998**, *552*, 285−292.
(16) Boring, E.; Sabat, M.; Finn, M. G.; Grimes, R. N. *Organometallics* **1998**, *17*, 3865−3874.
(17) Chirik, P. J.; Dalleska, N. F.; Henling, L. M.; Bercaw, J. E. *Organometallics* **2005**, *24*, 2789−2794.
(18) Den Haan, K. H.; Deboer, J. L.; Teuben, J. H.; Spek, A. L.; Kojicprodic, B.; Hays, G. R.; Huis, R. *Organometallics* **1986**, *5*, 1726−1733.
(19) Schaverien, C. J.; Vanderheijden, H.; Orpen, A. G. *Polyhedron* **1989**, *8*, 1850−1852.
(20) Van der Heijden, H.; Schaverien, C. J.; Orpen, A. G. *Organometallics* **1989**, *8*, 255−258.
(21) Schaverien, C. J.; Nesbitt, G. J. *J. Chem. Soc., Dalton Trans.* **1992**, 157−167.
(22) Klooster, W. T.; Brammer, L.; Schaverien, C. J.; Budzelaar, P. H. M. *J. Am. Chem. Soc.* **1999**, *121*, 1381−1382.
(23) Hitchcock, P. B.; Lappert, M. F.; Smith, R. G.; Bartlett, R. A.; Power, P. P. *J. Chem. Soc., Chem. Commun.* **1988**, 1007−1009.
(24) Van Der Sluys, W. G.; Burns, C. J.; Sattelberger, A. P. *Organometallics* **1989**, *8*, 855−857.
(25) Clark, D. L.; Gordon, J. C.; Hay, P. J.; Martin, R. L.; Poli, R. *Organometallics* **2002**, *21*, 5000−5006.
(26) Perrin, L.; Maron, L.; Eisenstein, O.; Lappert, M. F. *New J. Chem.* **2003**, *27*, 121−127.
(27) Brady, E. D.; Clark, D. L.; Gordon, J. C.; Hay, P. J.; Keogh, D. W.; Poli, R.; Scott, B. L.; Watkin, J. G. *Inorg. Chem.* **2003**, *42*, 6682−6690.
(28) Evans, W. J.; Drummond, D. K.; Zhang, H.; Atwood, J. L. *Inorg. Chem.* **1988**, *27*, 575−579.
(29) Tilley, T. D.; Andersen, R. A.; Zalkin, A. *Inorg. Chem.* **1984**, *23*, 2271−2276.
(30) Boncella, J. M.; Andersen, R. A. *Organometallics* **1985**, *4*, 205−206.
(31) Tilley, T. D.; Andersen, R. A.; Zalkin, A. *J. Am. Chem. Soc.* **1982**, *104*, 3725−3727.
(32) Clark, D. L.; Miller, M. M.; Watkin, J. G. *Inorg. Chem.* **1993**, *32*, 772−774.
(33) Roger, M.; Barros, N.; Arliguie, T.; Thuery, P.; Maron, L.; Ephritikhine, M. *J. Am. Chem. Soc.* **2006**, *128*, 8790−8802.
(34) Stewart, J. L.; Andersen, R. A. *Polyhedron* **1998**, *17*, 953−958.
(35) Eisenstein, O.; Maron, L. *J. Organomet. Chem.* **2002**, *647*, 190−197.
(36) Pantazis, D. A.; McGrady, J. E.; Maseras, F.; Etienne, M. *J. Chem. Theory Comput.* **2007**, *3*, 1329−1336.
(37) Flener-Lovitt, C.; Woon, D.; Dunning, T.; Girolami, G. S. *J. Phys. Chem. A* **2010**, *114*, 1843−1851.
(38) Pantazis, D. A.; McGrady, J. E.; Besora, M.; Maseras, F.; Etienne, M. *Organometallics* **2008**, *27*, 1128−1134.
(39) Etienne, M.; McGrady, J. E.; Maseras, F. *Coord. Chem. Rev.* **2009**, *253*, 635−646.
(40) Scherer, W.; Priermeier, T.; Haaland, A.; Volden, H. V.; McGrady, G. S.; Downs, A. J.; Boese, R.; Blaser, D. *Organometallics* **1998**, *17*, 4406−4412.
(41) Reed, A. E.; Weinstock, R. B.; Weinhold, F. *J. Chem. Phys.* **1985**, *83*, 735−746.

(42) Bader, R. F. W. *Atoms in Molecules: A Quantum Theory*; Clarendon Press: Oxford, 1990.
(43) Haaland, A.; Scherer, W.; Ruud, K.; McGrady, G. S.; Downs, A. J.; Swang, O. *J. Am. Chem. Soc.* **1998**, *120*, 3762−3772.
(44) Braga, D.; Grepioni, F.; Tedesco, E.; Biradha, K.; Desiraju, G. R. *Organometallics* **1997**, *16*, 1846−1856.
(45) Yang, X. M.; Stern, C. L.; Marks, T. J. *J. Am. Chem. Soc.* **1994**, *116*, 10015−10031.
(46) Maseras, F.; Crabtree, R. H. *Inorg. Chim. Acta* **2004**, *357*, 345−346.
(47) Bader, R. F. W.; Matta, C. F. *Inorg. Chem.* **2001**, *40*, 5603−5611.
(48) Vigalok, A.; Milstein, D. *Acc. Chem. Res.* **2001**, *34*, 798−807.
(49) Jaffart, J.; Etienne, M.; Reinhold, M.; McGrady, J. E.; Maseras, F. *Chem. Commun.* **2003**, 876−877.
(50) Jaffart, J.; Cole, M. L.; Etienne, M.; Reinhold, M.; McGrady, J. E.; Maseras, F. *Dalton Trans.* **2003**, 4057−4064.
(51) Tomaszewski, R.; Hyla-Kryspin, I.; Mayne, C. L.; Arif, A. M.; Gleiter, R.; Ernst, R. D. *J. Am. Chem. Soc.* **1998**, *120*, 2959−2960.
(52) Koetzle, T. F. *Trans. Am. Crystallogr. Assoc.* **1995**, *31*, 57−68.
(53) The orbital overlap in $TiEtCl_3(dmpe)$ was originally studied by Haaland, A.; Scherer, W.; Ruud, K.; McGrady, S.; Downs, A. J.; Swang, O. *J. Am. Chem. Soc.* **1998**, *120*, 3762−3772. We repeated their calculations using PBE0 and obtained essentially identical results.
(54) Thakur, T. S.; Desiraju, G. R. *J. Mol. Struct.* **2007**, *810*, 143−154.
(55) Reed, A. E.; Weinhold, F. *J. Chem. Phys.* **1983**, *78*, 4066−4073.
(56) Wrackmeyer, B.; Weidinger, J.; Milius, W. *Z. Anorg. Allg. Chem.* **1998**, *624*, 98−102.
(57) Cooper, A. C.; Clot, E.; Huffman, J. C.; Streib, W. E.; Maseras, F.; Eisenstein, O.; Caulton, K. G. *J. Am. Chem. Soc.* **1998**, *121*, 97−106.
(58) Ujaque, G.; Cooper, A. C.; Maseras, F.; Eisenstein, O.; Caulton, K. G. *J. Am. Chem. Soc.* **1998**, *120*, 361−365.
(59) Cooper, A. C.; Clot, E.; Huffman, J. C.; Streib, W. E.; Maseras, F.; Eisenstein, O.; Caulton, K. G. *J. Am. Chem. Soc.* **1999**, *121*, 97−106.
(60) van der Boom, M. E.; Iron, M. A.; Atasoylu, O.; Shimon, L. J. W.; Rozenberg, H.; Ben-David, Y.; Konstantinovski, L.; Martin, J. M. L.; Milstein, D. *Inorg. Chim. Acta* **2004**, *357*, 1854−1864.
(61) Kornblum, N.; Pinnick, H. W. *J. Org. Chem.* **1972**, *37*, 2050−2051.
(62) Brumaghim, J. L.; Priepot, J. G.; Girolami, G. S. *Organometallics* **1999**, *18*, 2139−2144.
(63) See the Supporting Informaion for full Gaussian reference.
(64) Hehre, W. J.; Ditchfield, R.; Pople, J. A. *J. Chem. Phys.* **1972**, *56*, 2257−2261.
(65) Hay, P. J.; Wadt, W. R. *J. Chem. Phys.* **1985**, *82*, 270−283.
(66) Wadt, W. R.; Hay, P. J. *J. Chem. Phys.* **1985**, *82*, 284−298.
(67) Check, C. E.; Faust, T. O.; Bailey, J. M.; Wright, B. J.; Gilbert, T. M.; Sunderlin, L. S. *J. Phys. Chem. A* **2001**, *105*, 8111−8116.
(68) Becke, A. D. *J. Chem. Phys.* **1993**, *98*, 5648−5652.
(69) Lee, C.; Yang, W.; Parr, R. G. *Phys. Rev. B* **1988**, *37*, 785−789.
(70) Perdew, J. P.; Burke, K.; Ernzerhof, M. *Phys. Rev. Lett.* **1996**, *77*, 3865−3868.
(71) Zhao, Y.; Schultz, N. E.; Truhlar, D. G. *J. Chem. Phys.* **2005**, *123*, 161103/1−4.